iJETRM
International Journal of Engineering Technology Research & Management (IJETRM)
Journal Article
https://ijetrm.com/issue/

EFFECT OF TOOL ROTATIONAL SPEED ON MICROSTRUCTURAL EVOLUTION AND HARDNESS OF SIC-REINFORCED DISSIMILAR FRICTION STIR WELDED AA6061 AND AA2017 ALLOYS

Jagannati Venumurali[1], M. Maruthi rao[1], S. Praveena[2], [3]B. Harshavardhan, M. Anil Kumar naik, N. Abubakar, G. H. Hari Prasad, M. Hemanth Reddy
[1,] Associate Professor, [2]Assistant Professor, [3]UG Students
Department of Mechanical Engineering, Annamacharya Institute of Technology and Sciences, Tirupati-517520, India
[*] murali.iskapalem502@gmail.com,

ABSTRACT
This study investigates the fabrication and characterization of silicon carbide (SiC) reinforced dissimilar friction stir welded (FSW) joints between AA6061-T6 and AA2017 aluminum alloys. Dissimilar joining of these alloys is critical for aerospace and automotive applications to leverage their complementary strength and weldability characteristics. SiC particles (40–50 µm) were integrated into a pre-machined groove at the joint interface to enhance microstructural refinement and mechanical performance. The welding process was executed at rotational speeds ranging from 1100 to 1500 rpm with a constant traverse speed of 20 mm/min. Results indicate that intermediate rotational speeds of 1300 rpm (FSW-3) and 1400 rpm (FSW-4) produced sound, defect-free joints, whereas extreme speeds led to tunneling defects or excessive flash formation. Microstructural analysis via optical and scanning electron microscopy revealed a highly refined, equiaxed grain structure in the stir zone (SZ) due to continuous dynamic recrystallization. The addition of SiC particles facilitated grain boundary pinning, further enhancing local hardness. Vickers microhardness profiles exhibited a characteristic "W-shape," with peak values occurring in the SZ. Sample FSW-3 achieved the highest hardness of approximately 103 HV, outperforming FSW-4 due to optimized thermal-mechanical equilibrium that prevented excessive grain growth and precipitate dissolution. The study concludes that precise control of rotational speed is essential for maximizing the strengthening effects of SiC reinforcement in dissimilar aluminum joints.

Keywords:
Friction Stir Welding; Dissimilar Joining; AA6061-AA2017; SiC Reinforcement; Microstructure; Vickers Microhardness

1. INTRODUCTION

Aluminum alloys from the Al–Mg–Si (AA6xxx) and Al–Cu (AA2xxx) series are extensively used in aerospace, automotive, and structural applications due to their high strength-to-weight ratio and good formability [1–3]. Among these, AA6061 is well known for its excellent weldability and balanced mechanical properties, whereas AA2017 exhibits higher strength and fatigue resistance due to the presence of Al_2Cu precipitates [4–6]. Dissimilar joining of these alloys is of significant engineering interest, as it enables the combination of their complementary properties within a single structure.

The strengthening mechanisms of AA6061 and AA2017 differ due to their alloy chemistry. AA6061 derives its strength primarily from Mg_2Si precipitates, while AA2017 is strengthened by Al_2Cu phases formed during age hardening [7,8]. However, conventional fusion welding of such dissimilar alloys often results in metallurgical issues such as the formation of brittle intermetallic compounds, segregation, and solidification defects, which degrade joint performance [9,10]. Furthermore, the thermal cycles involved in fusion welding can lead to the dissolution or coarsening of strengthening precipitates, causing localized softening in the heat-affected zone (HAZ) [11]. Friction stir welding (FSW), a solid-state joining technique, has emerged as an effective alternative to overcome these limitations. In this process, a rotating non-consumable tool generates frictional heat and plastic deformation, enabling material flow and bonding below the melting temperature [12]. This avoids solidification-related defects and promotes dynamic recrystallization, leading to the formation of a fine and equiaxed grain structure in the stir zone [13]. Consequently, FSW joints generally exhibit superior mechanical properties compared to those produced by conventional fusion welding techniques.

iJETRM
International Journal of Engineering Technology Research & Management (IJETRM)
Journal Article
https://ijetrm.com/issue/

To further enhance joint performance, recent studies have explored the incorporation of reinforcement particles into the weld zone during FSW. Ceramic reinforcements such as silicon carbide (SiC), Al_2O_3, and TiC have demonstrated significant improvements in microstructural refinement and mechanical properties [14,15]. Among these, SiC particles are particularly advantageous due to their high hardness, thermal stability, and compatibility with aluminum matrices. The addition of SiC particles restricts grain boundary movement through a pinning effect, resulting in refined grain structures and improved hardness. The distribution of reinforcement particles and the resulting microstructure are strongly influenced by FSW process parameters such as tool rotational speed, traverse speed, and tool geometry. Proper optimization of these parameters ensures uniform dispersion of particles and minimizes defects such as clustering or void formation. The refined microstructure achieved through the incorporation of SiC particles contributes directly to enhanced hardness and strength of the welded joints.

Despite the advantages of reinforced FSW, limited studies have been reported on SiC-reinforced dissimilar joints between AA6061 and AA2017 alloys, particularly with emphasis on microstructural characterization and hardness evaluation. Therefore, the present study focuses on the fabrication of SiC-reinforced dissimilar FSW joints between AA6061 and AA2017 alloys. Detailed microstructural analysis using optical microscopy and scanning electron microscopy (SEM) is carried out to examine grain refinement and particle distribution. In addition, hardness measurements are performed to evaluate the strength characteristics of the welded joints. This work aims to establish a clear relationship between reinforcement, microstructure, and mechanical performance in dissimilar FSW joints.

2. Experimental Procedure

AA6061-T6 and AA2017 plates with dimensions of 100 mm × 50 mm × 6.5 mm were used as base materials for the present investigation. The chemical composition and mechanical properties of both alloys were adopted from standard literature [1–3]. Prior to welding, square butt joints were prepared, and a narrow groove of approximately 2 mm depth and 1 mm width was machined along the joint interface to accommodate reinforcement particles. Silicon carbide (SiC) particles of micron size were introduced into the groove at the joint interface to examine their influence on the weld characteristics. The particles, with an average size in the range of 40–50 μm, were uniformly filled into the groove (**Fig.1(b)**) without specifying any particular weight percentage.

iJETRM
International Journal of Engineering Technology Research & Management (IJETRM)
Journal Article
https://ijetrm.com/issue/

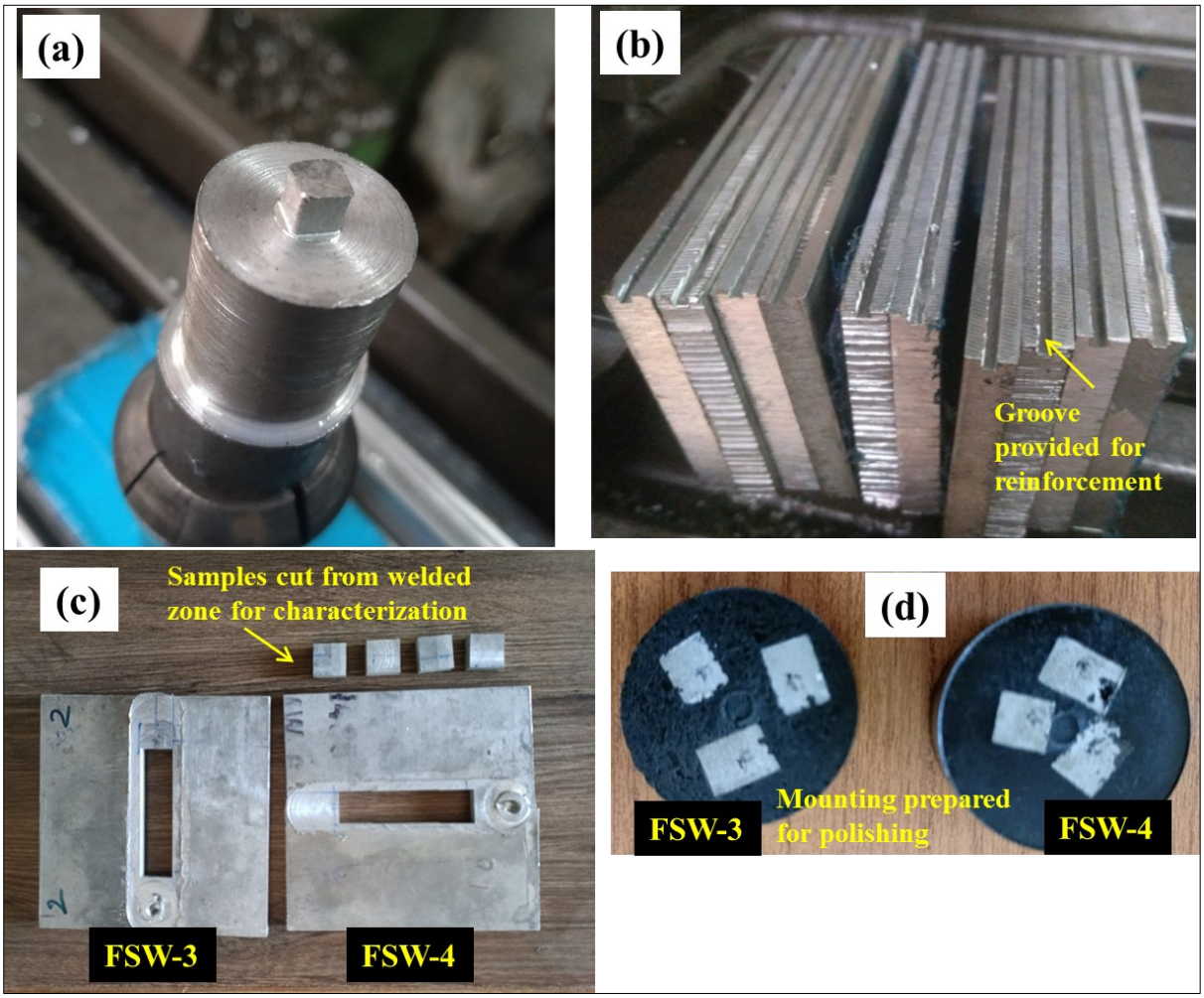

Fig. 1 FS welding components (a) FSW tool with square pin, (b) Aluminium plates made with grooves to retain reinforcement (c) FS Welded plates cut to extract the samples (d) Samples fixed in mount for characterization.

Friction stir welding was carried out using a vertical milling machine equipped with a non-consumable hot work tool steel (H13) tool. A square pin profile was employed, with a pin side length of 5.5 mm, a pin length of 6.3 mm (slightly less than the 6.5 mm plate thickness), and a shoulder diameter of 15 mm as show in **Fig 1(a).** Friction stir welding was performed by varying the rotational speed in the range of 1100–1500 rpm, while keeping the traverse speed constant at 20 mm/min and the tool tilt angle at 1° which are shown in **Table 1**.

Table 1: Friction Stir Welding Parameters

S. No.	Sample ID	Rotational Speed (rpm)	Traverse Speed (mm/min)	Tool Tilt Angle (°)
1	FSW-1	1100	20	1
2	FSW-2	1200	20	1
3	**FSW-3**	**1300**	**20**	**1**
4	**FSW-4**	**1400**	**20**	**1**
5	FSW-5	1500	20	1

The weld quality strongly depended on the rotational speed under the constant traverse speed (20 mm/min) and tool tilt angle (1°). Among the conditions, FSW-3 (1300 rpm) and FSW-4 (1400 rpm) exhibited sound and defect-free joints, indicating optimal heat input and material flow. In contrast, FSW-1 (1100 rpm) and FSW-2

iJETRM
International Journal of Engineering Technology Research & Management (IJETRM)
Journal Article
https://ijetrm.com/issue/

(1200 rpm) showed insufficient plasticization, leading to tunnel defects and lack of bonding. At the highest speed, FSW-5 (1500 rpm), excessive heat input resulted in flash formation and possible grain coarsening. Thus, intermediate rotational speeds provided balanced thermal and mechanical conditions for defect-free welding. Hence FSW-3 and FSW-4 were taken for characterizing the microstructural and microhardness features for this present work.

Further, the welded specimens were sectioned perpendicular to the welding direction to observe the transverse cross-section of the joint shown in **Fig. 1(c)**. The samples were mounted using hot mounting in a Buehler SimpliMet 4000 Mounting Press, followed by grinding with SiC papers (320 to 2000 grit) and polishing using diamond paste on a Buehler EcoMet 300 Grinder-Polisher to obtain a mirror-like surface finish. Final polishing was carried out using colloidal silica. The polished samples were etched with aqua regia to reveal the microstructure. Microstructural observations were performed using an optical microscope (Olympus GX53 Optical Microscope) to analyze the stir zone (SZ), thermo-mechanically affected zone (TMAZ), and heat-affected zone (HAZ). In addition, the Microhardness measurements were carried out using a Vickers microhardness tester (Mitutoyo HM-200 Vickers Microhardness Tester). A load of 500 g with a dwell time of 15 s was applied. Indentations were placed along the transverse cross-section at the mid-thickness with an interval of 0.5–1 mm, covering the base metal, HAZ, TMAZ, and SZ. The hardness profile was plotted to assess the variation in mechanical properties across the weld zones.

3. RESULTS AND DISCUSSION

3.1. Microstructural Evolution and Morphological Analysis

The microstructural characteristics of the friction stir welded (FSW) joints are primarily governed by the thermal-mechanical cycles experienced during the process. As illustrated in the optical micrographs (**Fig. 2(a-b)**) and SEM images (**Fig. 2(c-d)**), the Stir Zone (SZ) of samples FSW-3 and FSW-4 exhibits a highly refined, equi-axed grain structure. This morphology is a direct consequence of continuous dynamic recrystallization (CDRX), triggered by the intense plastic deformation and frictional heating induced by the rotating tool pin [16]. The transition from the base metal's coarse grains to the fine-grained SZ is critical for enhancing the joint's mechanical integrity.

At a rotational speed of 1300 rpm (FSW-3), the heat input is sufficient to facilitate adequate material flow and plasticization, resulting in a dense microstructure free of macroscopic defects such as unnelling or "lazy S" features. When the speed is increased to 1400 rpm (FSW-4), the SEM analysis (**Fig. 2©**) reveals a more homogeneous distribution of secondary phase particles within the matrix. This improved dispersion is attributed to the increased peak temperature and higher strain rates, which effectively fragment and redistribute constituent particles [17]. However, a subtle coarsening of grains is observed in FSW-4 compared to FSW-3, indicating that while higher speeds improve material mixing, they also extend the cooling cycle, allowing for slight grain growth.

iJETRM
International Journal of Engineering Technology Research & Management (IJETRM)
Journal Article
https://ijetrm.com/issue/

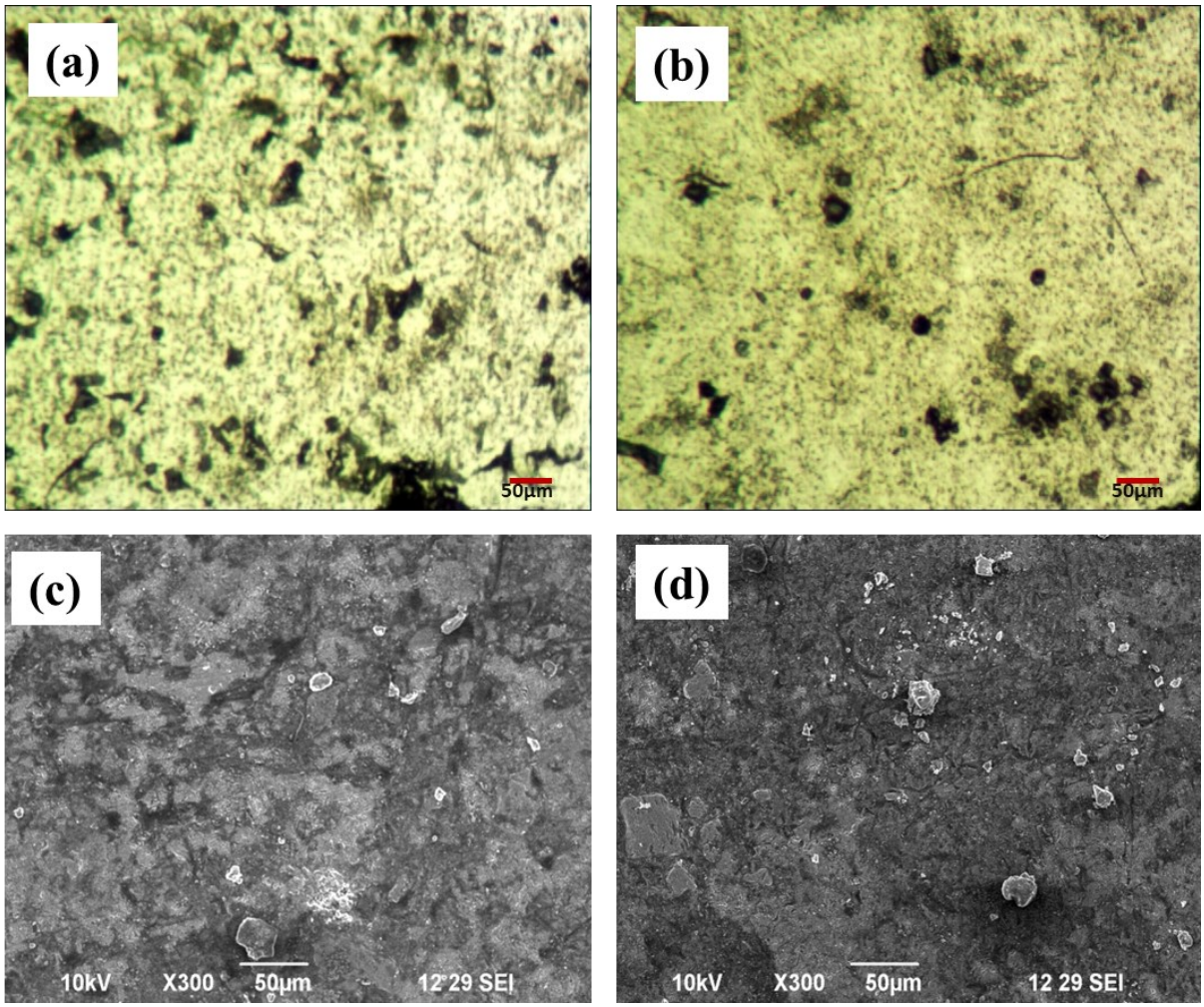

Fig. 2 Microstructure of FS welded joints by Optical micrographs (a) FSW-3, (b) FSW-4 and SEM images (c) FSW-3, (d) FSW-4.

The boundary between the SZ and the Thermo-Mechanically Affected Zone (TMAZ) shows highly elongated and deformed grains, reflecting the localized shear stress that was insufficient to trigger full recrystallization. In contrast, the Heat Affected Zone (HAZ) undergoes purely thermal cycles, often leading to precipitate over-aging or dissolution, which typically corresponds to the minimum hardness values observed in the transverse microhardness profiles [18]. The microstructural observations confirm that the intermediate rotational speeds (1300–1400 rpm) achieve an optimal "thermal-mechanical equilibrium," producing defect-free joints with superior grain refinement and phase distribution compared to the insufficient plasticization seen at lower speeds or the excessive flash formation at 1500 rpm.

3.2. Microhardness distribution in the Stir Zone (SZ)

The microhardness distribution across the cross-section of the friction stir welded (FSW) joints for samples FSW-3 (1300 rpm) and FSW-4 (1400 rpm) is illustrated in the provided figure, revealing a profile characteristic of the FSW process across the Stir Zone (SZ), Thermo-Mechanically Affected Zone (TMAZ), and Heat-Affected Zone (HAZ). Both samples exhibit peak hardness values within the SZ, located near the weld center (0 mm to ±2.5 mm), where FSW-3 reaches approximately 103 HV. This localized hardening is primarily attributed to the finer grain structure resulting from dynamic recrystallization; according to the Hall-Petch relationship, this grain refinement increases the density of boundaries that impede dislocation movement. However, a distinct downward shift in the hardness profile is observed as the rotational speed increases to 1400 rpm. While the higher speed improves material flow, it simultaneously increases the heat input, which in the case of FSW-4 promotes marginal grain growth and the coarsening or dissolution of strengthening precipitates. Consequently,

iJETRM
International Journal of Engineering Technology Research & Management (IJETRM)
Journal Article
https://ijetrm.com/issue/

FSW-4 consistently maintains lower hardness values—typically 2–5 HV points below FSW-3 across the entire profile.

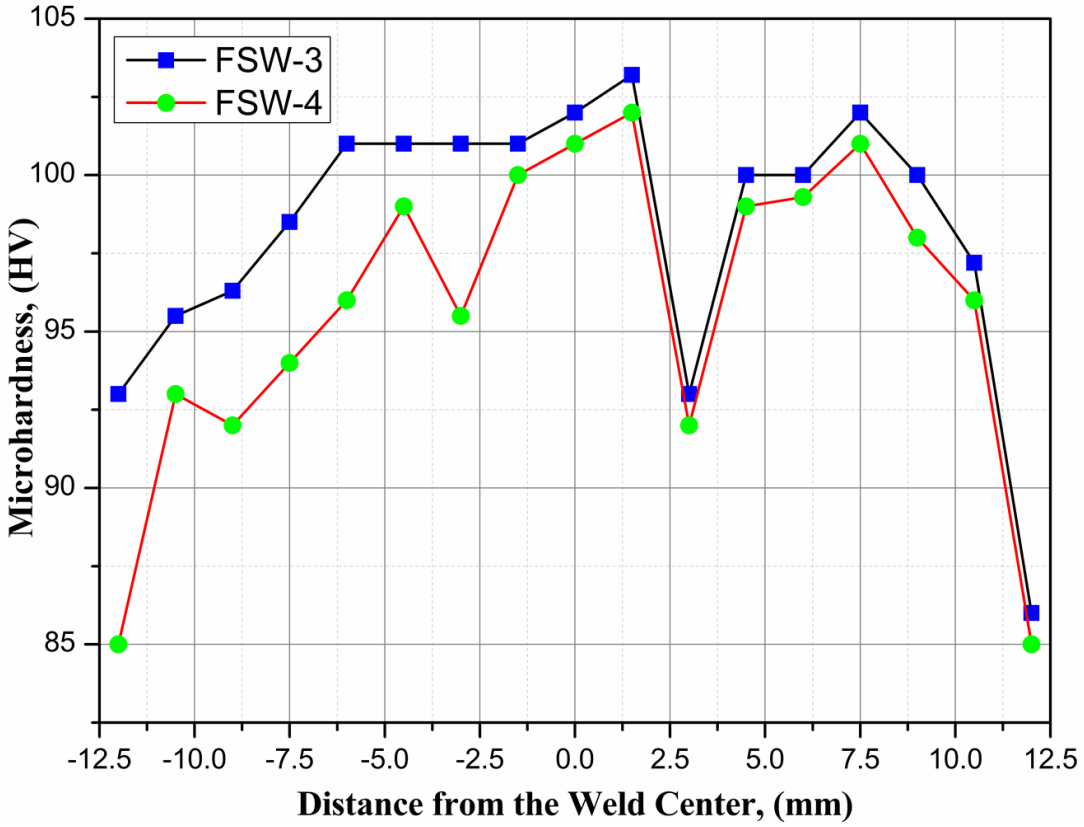

Fig. 3 Microhardness distribution in the Stir Zone of FS welded joints FSW-3 and FSW-4.

Moving away from the weld centre beyond ±7.5 mm, both samples show a significant drop in hardness toward 85 HV within the HAZ. This "softening" is a typical phenomenon in heat-treatable aluminium alloys, driven by the over-aging of precipitates during the thermal cycle. The fluctuations observed between ±3 mm and ±6 mm represent the complex transition zones where plastic deformation and thermal gradients vary sharply. Ultimately, the data indicates that FSW-3 provides a superior mechanical profile, suggesting that 1300 rpm offers the optimal balance between mechanical stirring and thermal management to preserve the structural integrity of the joint.

4. CONCLUSIONS

In the present work, FSW was successfully applied to join AA6061 and AA2017 with the incorporation of SiC reinforcement particles. The microstructure and microhardness behavior of the joints were analyzed. The results can be summarized as follows:

- Successful dissimilar joining of AA6061 and AA2017 with SiC reinforcement was achieved using friction stir welding, with optimal results observed at intermediate rotational speeds.
- Rotational speeds of 1300 rpm and 1400 rpm produced defect-free joints, while lower speeds (1100–1200 rpm) resulted in insufficient plasticization and tunneling defects.
- The Stir Zone exhibited significant grain refinement and a dense, equiaxed microstructure attributed to continuous dynamic recrystallization and the pinning effect of SiC particles.
- Microhardness distribution confirmed that sample FSW-3 (1300 rpm) provided superior mechanical integrity, reaching a peak of 103 HV, whereas the higher heat input in FSW-4 (1400 rpm) led to a hardness reduction of 2–5 HV due to precipitate coarsening.
- Significant softening was observed in the Heat-Affected Zone (HAZ), with hardness dropping to approximately 85 HV due to the over-aging of strengthening precipitates during the thermal cycle.

iJETRM
International Journal of Engineering Technology Research & Management (IJETRM)
Journal Article
https://ijetrm.com/issue/

- Based on the promising microhardness results and the observed microstructural refinement, it is scientifically recommended to conduct further mechanical evaluations, including tensile testing and wear resistance analysis, to comprehensively establish the future scope and industrial viability of these reinforced dissimilar joints.

REFERENCES

1) Jung J, Cho YJ, Kim SH, Lee YS, Kim HJ, Lim CY, Park YH (2020). Microstructural and mechanical responses of various aluminum alloys to ballistic impacts by armor piercing projectile. Materials Characterization, 159, 110033. https://doi.org/10.1016/j.matchar.2019.110033
2) Engler O, Hirsch J (2002). Texture control by thermomechanical processing of AA6xxx Al–Mg–Si sheet alloys for automotive applications—A review. Materials Science and Engineering A, 336(1–2), 249–262. https://doi.org/10.1016/S0921-5093(01)01968-2
3) Mukhopadhyay P (2012). Alloy designation, processing, and use of AA6XXX series aluminium alloys. ISRN Materials Science, 2012, 165082. https://doi.org/10.5402/2012/165082
4) Sabry I, El-Kassas AM (2017). A comparison between FSW, MIG, and TIG based on total cost estimation for aluminum pipes. European Journal of Advances in Engineering and Technology, 4(3), 158–163.
5) Khourshid AM, Sabry I (2013). Friction stir welding study on aluminum pipe. International Journal of Mechanical Engineering and Robotics Research, 2(3), 331–339.
6) Zhang W, Xu J (2022). Advanced lightweight materials for automobiles: A review. Materials & Design, 221, 110994. https://doi.org/10.1016/j.matdes.2022.110994
7) Hammad AS, Lu H, Seleman MM El-Sayed, et al. (2022). Optimization of friction stir welding AA6082-T6 parameters using ANOVA and grey relational analysis. Journal of Physics: Conference Series, 2299(1), 012015. https://doi.org/10.1088/1742-6596/2299/1/012015
8) Sabry I, El-Zathry NE, Hewidy AM (2022). Experimental investigation on joining process of aluminum alloy 6082-T6 (plate to pipe) using friction stir welding. Proceedings of NILES 2022, 360–363. https://doi.org/10.1109/NILES56402.2022.9942413
9) Sabry I, Singh VP, Mourad AHI, Hewidy A (2024). Flange joining using FSW and TIG of AA6082: A comparison based on joint performance. International Journal of Lightweight Materials and Manufacture, 7(5), 688–698. https://doi.org/10.1016/j.ijlmm.2024.05.001
10) Sabry I, Thomas Thekkuden D, Mourad AHI, Husain Khan S (2022). Optimization of TIG welding parameters for AA6082 pipes using grey relational analysis. ASET 2022 Conference Proceedings. https://doi.org/10.1109/ASET53988.2022.9735100
11) Rebrin M et al. (2024). Ultrasound-enhanced friction stir welding of aluminum alloy 6082: Advancements in mechanical properties and microstructural refinement. Metals, 14(11), 1241. https://doi.org/10.3390/met14111241
12) Wakchaure K et al. (2023). Effect of cooling temperature on microstructure and mechanical properties of Al 6061-T6 during submerged FSW. Metals, 13(7), 1159. https://doi.org/10.3390/met13071159
13) Sabry I et al. (2024). Effect of rotational speed and penetration depth on Al–Mg–Si welded T-joints in underwater and conventional FSW. Journal of Advanced Joining Processes, 9, 100207. https://doi.org/10.1016/j.jajp.2024.100207
14) Sabry I et al. (2019). Friction stir welding of T-joints: Experimental and statistical analysis. Journal of Manufacturing and Materials Processing, 3(2), 38. https://doi.org/10.3390/jmmp3020038
15) El-Kassas AM, Sabry I, Mourad AHI, Thekkuden DT (2019). Characteristics of vertical force, torque, and current on penetration depth in FSW of AA6061 pipes. International Review of Aerospace Engineering, 12(4), 195–204. https://doi.org/10.15866/irease.v12i4.16362
16) Mishra RS, Ma ZY (2005). Friction stir welding and processing. Materials Science and Engineering: R: Reports, 50(1-2), 1–78. https://doi.org/10.1016/j.mser.2005.07.001
17) **Sato YS, Kokawa H, Enomoto M, Jogan S (1999).** Microstructural evolution of 6063 aluminum during friction stir welding. *Metallurgical and Materials Transactions A*, 30(9), 2429–2437. https://doi.org/10.1007/s11661-999-0251-1
18) **Heidarzadeh A, et al. (2021).** A review of friction stir welding of metals and alloys: Process, structure, and properties. *Progress in Materials Science*, 117, 100752. https://doi.org/10.1016/j.pmatsci.2020.100752